Archives of Hydro-Engineering and Environmental Mechanics
Vol. 56 (2009), No. 1–2, pp. 29–41

The Simultaneous Occurrence of Logarithmic and S-Shaped Velocity Profiles in Gravel-Bed River Flows

Mário J. Franca[1], Urlich Lemmin[2]

[1]FCT – New University of Lisbon and IMAR-CMA (Un. Coimbra)
Quinta da Torre, 2829-516 Caparica, Portugal,
e-mail: mfranca@fct.unl.pt (corresponding author)
[2]ENAC, École Polytechnique Fédérale de Lausanne
CH 1015 Lausanne, Switzerland,
e-mail: ulrich.lemmin@epfl.ch

(Received December 17, 2008; revised July 19, 2009)

Abstract

Based on Acoustic Doppler Velocity Profiler (ADVP) field measurements, we discuss velocity profiles observed in two shallow gravel-bed rivers with low relative submergence. In these flows, log-shaped profiles and s-shaped profiles simultaneously exist, indicating the possibility of 3D flow inside the roughness layer. A quasi-2D layer is generally found in an intermediate region of the flow above the roughness layer. Therefore a best-fit log-law approach may lead to estimates of a roughness parameter which are reasonably correlated with the local flow resistance. However, above a certain limit of the ratio roughness/water depth (≈ 0.6 from our measurements), the velocity distribution in the lower regions predominantly corresponds to an s-shaped profile.

Key words: field measurements; gravel-bed river flows; velocity profiles

1. Introduction

Most open-channel concepts are based on laboratory experiments. In order to validate them in rivers, field measurements have to be carried out. Unfortunately, only a limited number of field studies exist which may be due to the difficulty in obtaining reliable measurements with existing instrumentation. The logarithmic profile approach is often used to describe the mean velocity distribution in boundary layer flows (Monin and Yaglom 1971). However, in the lower layers of shallow flows over rough surfaces found in rivers, bottom roughness may affect the development of the log-shaped velocity profile. Nikora and Smart (1997) found deviations from the log-law flow in the roughness layer which is a 3D inner layer of the flow in gravel-bed rivers. In such flows, a velocity inflection has been observed, resulting in so-called s-shaped profiles (Marchand et al 1984, Bathurst 1988 and Ferro and

Baiamonte 1994). In most cases, these deviations are due to the wake effect resulting from the presence of bed forms, gravel clusters or large-scale roughness elements that deform the mean velocity profile as observed by Nelson et al (1993) and Buffin-Bélanger and Roy (1998). Their occurrence is thus local. In the case of an s-shaped profile, the streamwise momentum is concentrated in the upper layers of the flow where the velocity distribution becomes almost uniform (parallel streamlines) (Franca 2005a). Katul et al (2002) compared s-shaped profiles resulting from the drag effect on the canopy in atmospheric flows with s-shaped profiles observed in gravel-bed rivers.

These observations indicate that shear production in these rough-bed flows is no longer limited to a log-based layer near the bottom. This also affects the turbulence distribution due to the different forms of shear zones near the bottom. Based on Acoustic Doppler Velocity Profiler (ADVP) field measurements, we show that the application of a logarithmic profile in the description of the velocity distribution may still be valid for a large number of rough bed flow cases. However, in the measured profiles, the depth range of the region in which the logarithmic velocity distribution is found, may vary. Using the field data, it is demonstrated that the parameterization of a velocity profile by a logarithmic best-fit approach applied in the regions above the roughness layer may provide information on the velocity distribution within the lower layers of the flow, in particular on the occurrence of s-shaped profiles.

2. Field Work and Instrumentation

This study is based on two sets of field measurements carried out in the Swiss lowland rivers, Venoge and Chamberonne, both located in the canton of Vaud. The measurements were taken during the summer of 2003, under stationary shallow water conditions in straight river reaches. The measuring position for the Venoge was about 120 m upstream of the Moulin de Lussery and for the Chamberonne, 385 m upstream from the river mouth. The hydraulic characteristics of the two rivers during the measurement period are summarized in Table 1.

Table 1. Summary of the rivers' flow characteristics

River	i (%)	Q (m^3/s)	h (m)	W (m)	$Re = \overline{U}h/\nu$ ($\times 10^4$)	$Fr = \overline{U}/\sqrt{gh}$	u^* (mm)	D_{50} (mm)	D_{84}/D_{50}
Venoge	0.33	0.80	0.21	6.30	12.6	0.42	0.078	40	1.74
Chamberonne	0.26	0.55	0.25	5.75	9.5	0.24	0.085	49	1.65

where:

- i – river slope,
- Q – discharge,
- h – water depth,
- W – river width,
- Re – Reynolds number,
- $\overline{U}$ – vertically averaged streamwise velocity,
- ν – kinematic viscosity,
- Fr – Froude number,
- g – acceleration due to gravity,
- $u*$ – bottom friction velocity,
- D_n – bottom grain size diameter for which $n\%$ of the grain diameters are smaller (D_{50} and D_{84} were obtained from samples of the bed material).

The riverbed consisted of coarse gravel with randomly spaced macro-roughness elements. The gravel-bed material was sampled by the Wolman method (Wolman 1954). Based on the relative submergence defined as h/D_{50} of 5.25 and 5.10 for the Venoge and Chamberonne, respectively, the rivers are of intermediate scale roughness (Bathurst et al 1981). No sediment transport occurred during the measurements.

Quasi-instantaneous velocity profiles were measured across river sections in both cases. For the Venoge, 25 velocity profiles were taken, horizontally spaced with 10 to 12.5 cm distance; for the Chamberonne, 24 profiles were measured with horizontal spacing of 5 to 12.5 cm. Data were recorded for 5 minutes at each position. The deployable 3D ADVP developed at the EPFL was used to measure quasi-instantaneous full-depth 3D velocity profiles with high resolution in the vertical at each position. This system allows for an efficient collection of detailed velocity measurements which are needed to observe the shape of the velocity distribution throughout the depth with sufficient resolution. The ADVP system is described in Rolland and Lemmin (1997) and Shen and Lemmin (1997). In the present case, a multistatic ADVP configuration was used which provided instantaneous profiles of all three velocity components. In both measurements, the Pulse Repetition Frequency (PRF) was set to 2000 Hz for the Doppler shift estimates. A dealiasing algorithm was applied to the raw data allowing theoretically noise-free 3D velocity estimates (Franca and Lemmin 2006).

3. Results

3.1. Mean Velocity Vertical Distribution

For the river flows discussed here, Franca (2005b) found that the lower 40% of the profiles could be matched by a logarithmic profile in about 65% of the profiles taken. The river bottom level is taken as the shallowest point of the solid bed in the vertical of each measured profile. Often this may be the top of a rock or a boulder. The zero reference level is set at the water surface. In the parameterization of the logarithmic law, the dimensionless parameter B is taken as $B = 8.5$ (Monin and Yaglom 1971); B may also be considered as a geometry parameter in the log-law parameterization (Schlichting 1968).

In the remaining 35% of the profiles, deviations from the log-law occurred in the lower part of the flow. This near bottom layer may be defined as a roughness layer ($z < Z_{RL}$), where the flow is highly 3D and the mean velocity profile may deviate from the log-law shape (Nikora and Smart 1997). The upper limit of the roughness layer is formed by a 3D surface which follows the top of the local riverbed. In our case, as shown in Figs. 1a and 1b, the roughness layer may be defined by the limit $Z_{RL}/h \approx 0.30$. This scale is nearly equivalent to D_{75} of the grain size distribution.

3.2. Log-Shaped and S-Shaped Profiles in the Lower Layer of the Flow

Based on the velocity distribution in the lower layer, most of the measured velocity profiles fall into two groups: one with a log-shaped lower layer (36 profiles), and the other one with an s-shaped lower layer (13 profiles). The simultaneous occurrence but random distribution of these two types of velocity profiles in both river cross sections indicates that lateral momentum transfer exists in the lower layers of the flow and that a 3D inner layer has developed in the flow (Nikora and Smart 1997). A velocity deficit of about $\Delta U/U_{\max} \approx 0.20$ at $z/h = 0.10$ suggests that this lateral momentum exchange may be important (Fig. 1b). Here Δ indicates the difference or deficit in the time averaged velocity U between an expected logarithmic velocity profile and the real profile; subscript 'max' refers to the maximum in the profile. In both river flows, two zones can be identified in which significant lateral exchange of momentum takes place: the near bottom boundary layer, discussed in this paper, where log- and s-shaped profiles are simultaneously observed, and a near surface layer, where alternating higher and lower velocities in the cross section are found (Franca and Lemmin 2005). Between these two zones a layer exists, where no significant lateral exchange occurs.

Bathurst (1988) and Ferro and Baiamonte (1994) investigated the influence of bottom roughness on the shape of velocity profiles, taking as a parameter the depth/sediment size ratio, i.e. the inverse of a measure of the relative bottom roughness represented by a characteristic diameter (D_{84} and D_{50}). By using the representative diameters D_{50} and D_{84} (Fig. 2), the depth/sediment size ratios $h/D_{50} = 5.25$

a)

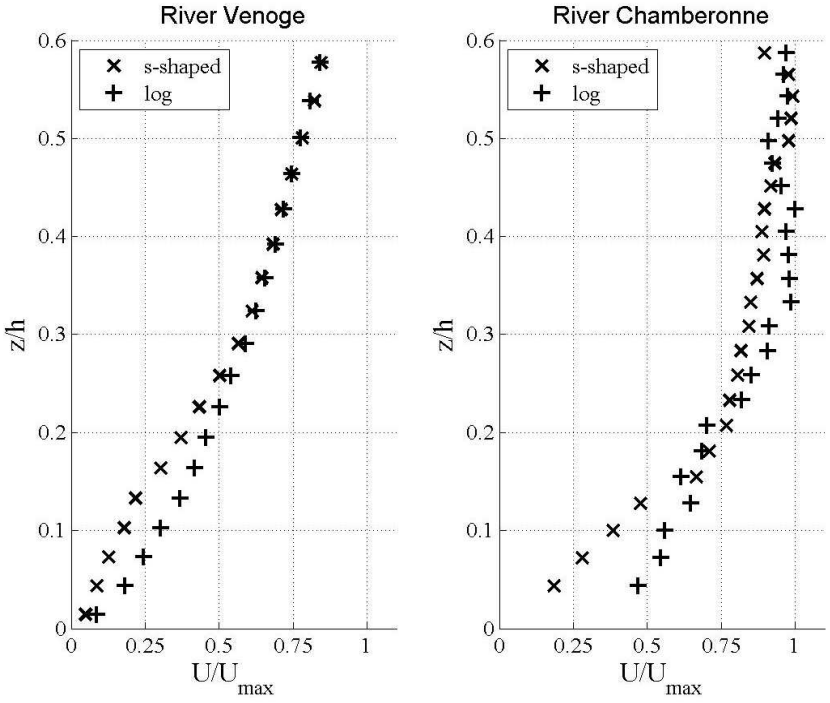

b)

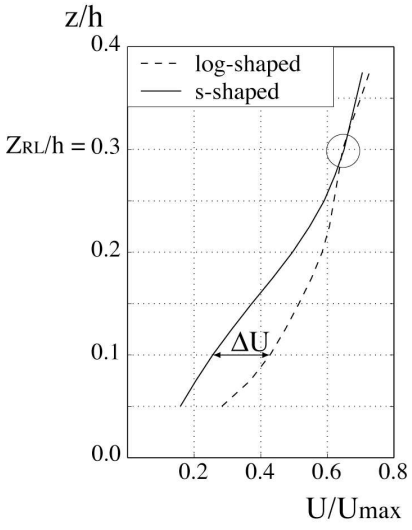

Fig. 1. (a) Examples of the two types of lower layer velocity distributions, s-shaped and log-shaped; the data correspond to time-averaged velocity profiles obtained for both rivers, normalized by the local maximum velocity, and (b) representation of the average mean velocity profiles normalized by the local maximum velocity corresponding to log-shaped and s-shaped lower layer profiles; circle: identification of the height of the roughness sublayer

and 5.10, and h/D_{84} = 3.02 and 3.09 are obtained for the Venoge and Chamberonne, respectively; these values are within the limits for the occurrence of s-shaped profiles given in the literature. However, in the present investigation, we observed that individual s-shaped velocity profiles are a consequence of local protrusions on the riverbed and that, different from the literature, they exist together with log-shaped profiles in the same river cross section.

A continuous grain size distribution is not found in the cross sections (Fig. 3), and thus continuity between two adjacent profiles may not exist. Unlike typical laboratory open- channel beds, changes in riverbed bottom roughness may be abrupt (Fig. 3), leading to non-uniform size distribution and 3D inner layers where the local equivalent roughness parameter is the result of an integration of local and upstream/lateral conditions. A general wake effect, as described by Morris (1959), which induces a lower region where form-drag from bed elements continuously deforms the velocity profile, is not found in these rivers.

Given the spatial variation of the velocity distribution and the coexistence of several types of profiles, mean grain size such as D_{50} or D_{84} may no longer be a relevant "bulk" parameter for characterizing the shape of the velocity profile in these rivers. Although the log law cannot describe the lower layer of all velocity profiles, a Nikuradse-type equivalent roughness parameter (k) obtained from a best-fit logarithmic law approach may still give an indication of the local roughness (Franca 2005b).

A relationship between the cumulative bed particle size distribution and the cumulative distribution of k values (Fig. 2) can be established from an analysis of k, obtained for both rivers independently, by a best-fit approach to logarithmic profiles. Two distinct cases occur in these rivers. In the Venoge river, both the grain size and the equivalent roughness distributions collapse for values beyond $D_{50} \approx k_{50}$ (k_{50} is the equivalent roughness for which 50% of the estimated values are smaller). In the Chamberonne river, both curves cross over only once for $D_{28} \approx k_{28}$. In this case, the grain diameter and the k value distribution do not coincide, but have similar slopes. For the Venoge, k varies between 1.5 mm and 119.5 mm, and between 5.0 mm and 212.8 mm for the Chamberonne. k_{50} corresponds to the values of D_{50} and D_{84} for the Venoge and Chamberonne rivers, respectively. Discrepancies occur for small grain sizes. This is to be expected, because the effects of the larger surrounding grains dominate in such a rough bed flow.

Therefore, we suggest that the roughness parameter values can be used to qualitatively map the local roughness of the riverbed. Fig. 4 shows the distribution of the local relative roughness ratio (k/h) for the log-shaped and s-shaped cases. The distinction between the two profile types was made by visual inspection. For higher relative roughness, we observe a slightly higher tendency for the occurrence of s-shaped profiles, in agreement with previous studies. It appears that $k/h \approx 0.5$–0.6 constitutes a limit above which the lower layer profiles become predominantly s-shaped. From the distribution of k values, it can be assumed that the roughness

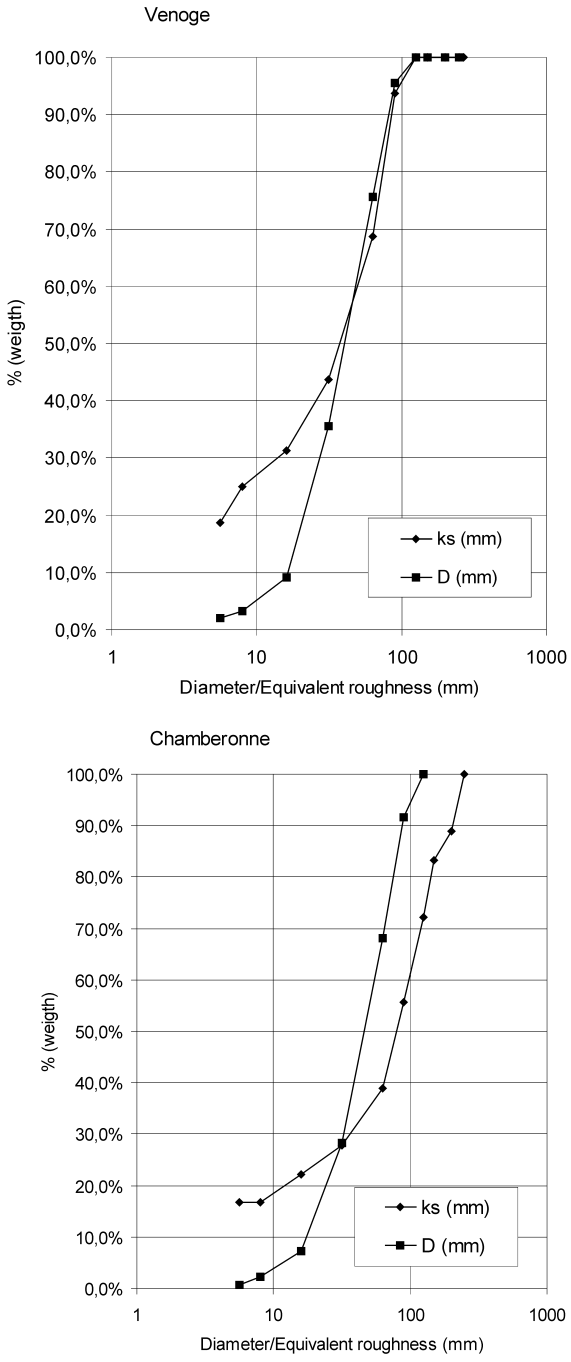

Fig. 2. Cumulative bed particle size distribution and cumulative distribution of k values for both rivers

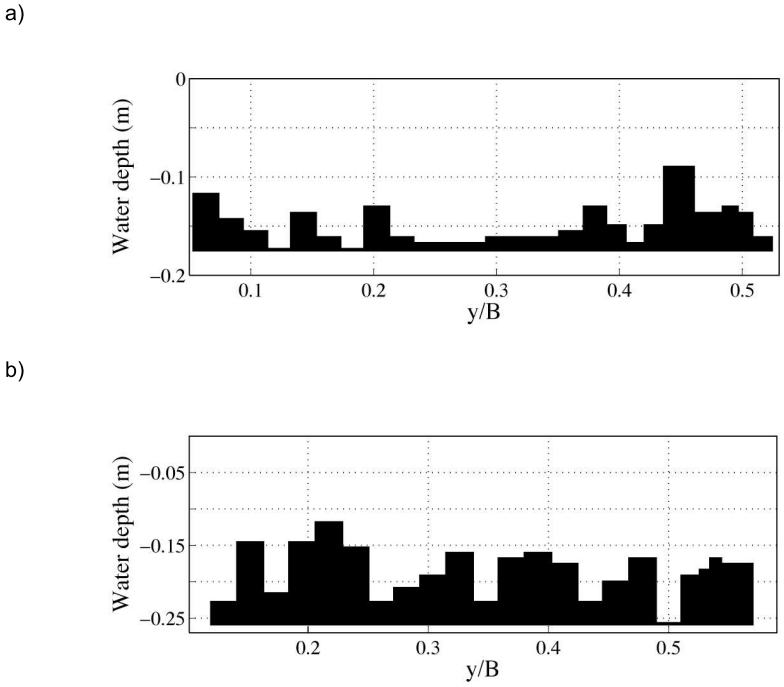

Fig. 3. Cross section bed profiles for the rivers (a) Venoge and (b) Chamberonne determined from the ADVP measurements and presented as step functions. Profiles are measured in the centre of each step

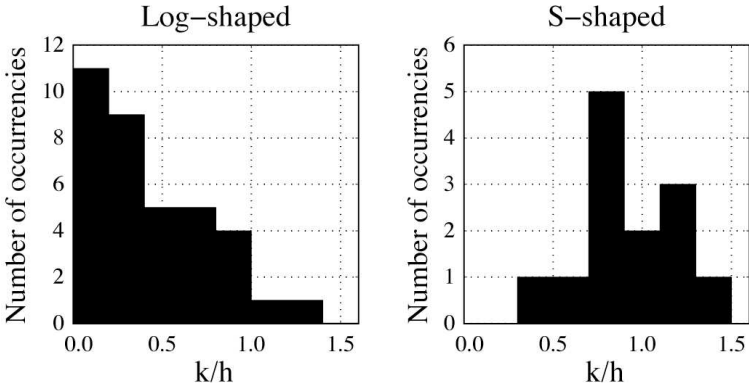

Fig. 4. Distribution of the relative roughness (k/h) for the case of log-shaped (left) and s-shaped (right) lower layer profiles. Note the change in vertical scales

parameter herein determined represents a measure of the wake effect in the velocity measurements which is locally felt, but actually caused by a combination of local grain size and upstream/lateral perturbations of the bottom.

In order to further investigate the s-shaped profile, the following two dimensionless parameters were calculated: the normalized velocity deficit between a log-law based profile and the measured profile, calculated for $z/h = 0.10$ (Fig. 1b), and the normalized lower-layer unit discharge deficit, calculated for $z/h < 0.30$.

$$\frac{\Delta U_{0.10}}{U_{\max}} = \frac{\left| U_{\log}\left(\frac{z}{h} = 0.10\right) - U_{meas}\left(\frac{z}{h} = 0.10\right)\right|}{U_{\max,meas}}, \tag{1}$$

$$\frac{\Delta q_{0.30}}{q} = \frac{\left| q_{\log}\left(\frac{z}{h} < 0.30\right) - q_{meas}\left(\frac{z}{h} < 0.30\right)\right|}{q_{meas}\left(\frac{z}{h} < 1.00\right)}, \tag{2}$$

where the subscript *log* relates to the log-law based profiles and the subscript *meas* refers to directly measured profiles. In Fig. 5, we plot these two non-dimensional parameters against the relative roughness. Log-shaped and s-shaped profiles, as identified above, are plotted with different symbols.

In both cases there is again a clear tendency for the occurrence of s-shaped profiles for $k/h > 0.5$–0.6. The points relating to s-shaped profiles have an increasing trend with relative roughness. This is more evident in the lower graph of Fig. 5 where the lower-layer unit discharge deficit ($\Delta q_{0.30}/q$) is presented. These results confirm that k can be used as a characteristic parameter for the determination of the occurrence of s-shaped profiles. Therefore, k characterizes local conditions associated with the occurrence of s-shaped velocity profiles. Bathurst (1988) and Ferro and Baiamonte (1994) had defined a "bulk" parameter based on a characteristic grain size related to the bed material to be applied on a continuous mean where the profile deformation is ubiquitous.

Although the influence of the roughness layer deviation is evident in the velocity profile analysis, it does not greatly affect the estimate of the local unit discharge. In Fig. 5b, we find a maximum error of less than 3% for these calculations. In terms of mean velocity deficit, the error made by using the log law is about 25% of the local maximum velocity, as shown in Fig. 5a.

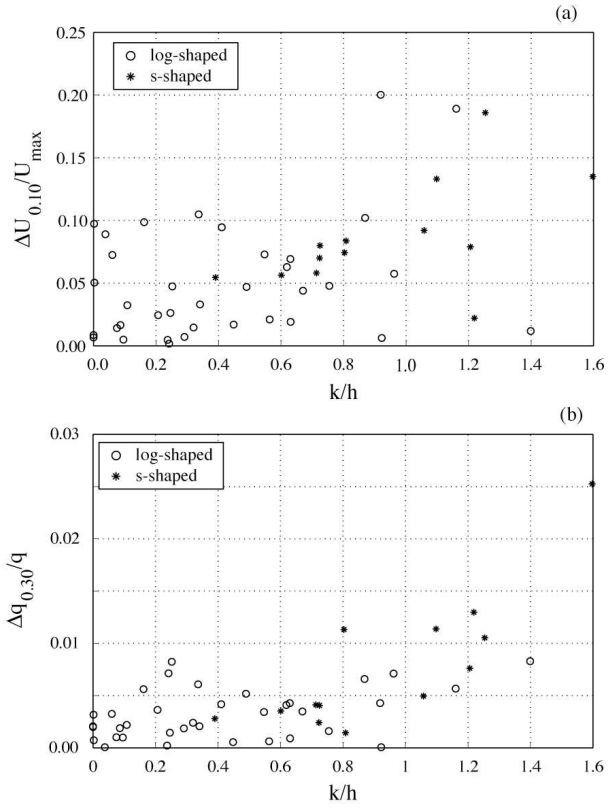

Fig. 5. (a) Normalized velocity deficit calculated for $z/h = 0.10$ plotted against *local* relative roughness, and (b) normalized low-layer unitary discharge deficit calculated for $z/h < 0.30$ plotted against *local* relative roughness

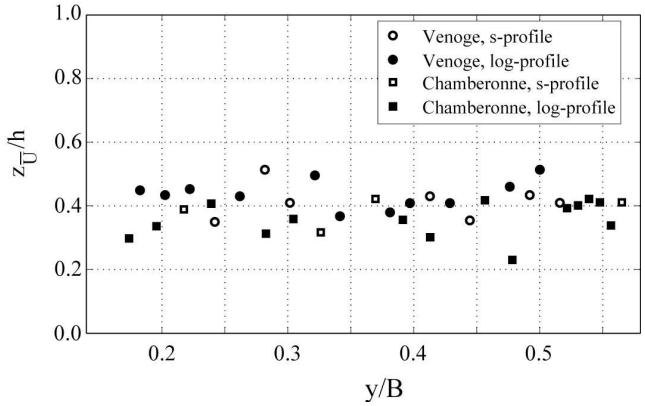

Fig. 6. Cross section distribution of $Z_{\overline{U}}$ normalized by the local water depth

4. Conclusions

In this paper, we discussed the occurrence of log-shaped and s-shaped velocity profiles measured in cross sections of two shallow gravel-bed river flows. Based on the observed depth/sediment size ratio, s-shaped profiles should dominate according to Ferro and Baiamonte (1994). However, log- and s-shaped velocity profiles simultaneously occurred in the lower layers of the flow in both river cross sections, indicating that the flow in the inner layer was organized in 3D. Since log-shaped profiles were more frequent in both rivers, mean sediment size is not necessarily a characteristic parameter uniquely determining the flow structure in rivers. A log layer can still be found in most s-shaped profiles, starting, however, at different heights above the bed.

In engineering practice, simple in-situ velocity measurements are often only taken at a few depths in the upper layers of the flow (typically at $z/h > 0.30$) due to the difficulties of measuring in the inner layer and to define a precise reference level. A logarithmic velocity distribution may be fitted through these points which provides a roughness parameter analogous to the Nikuradse equivalent roughness. This roughness parameter may serve as a qualitative indicator of the local roughness which is felt by the flow, because it integrates local, upstream and lateral effects which influence the local velocity profile. The local obstruction of the flow by the upstream presence of pebble clusters, large boulders or groups of large boulders within the stream, often extending to $h/D_{84} < 1$, may result in values of $k/h > 1$.

The log-law obtained by a best-fit approach to field data in the intermediate layers may then be used to predict the velocity distribution within the inner layers of the flow. For relative equivalent roughness values of $k/h > \approx 0.6$, we found that the velocity distribution in the lower layers is probably s-shaped and a logarithmic approach applied to the whole velocity profile is no longer valid. This agrees with previous studies (Bathurst 1988, Ferro and Baiamonte 1994) which used the depth to sediment size ratio (which may considered as a measure of the relative roughness) as a parameter to determine whether s-shaped profiles occur. We have shown here that k values and grain size are correlated, in particular for larger values. Therefore, the calculated k values can be related to a bulk bottom sediment size. In the future, the results of the present study will be used to determine the profile form, log- or s- shaped profiles, from less detailed profile measurements in the outer layer. Mean velocity point measurements in the outer layers of the flow are often easier to carry out than detailed mapping of the riverbed, particularly since discharge information can be obtained from velocity measurements at the same time.

For further identification of the different profile types, the local unit discharge deficit as herein defined may be used. However, errors in river flow modelling which may be caused by not considering s-shaped profiles are less severe in terms of local mass transfer than in terms of the vertical distribution of velocity (related to momentum transfer).

Acknowledgements

The authors acknowledge the financial support of the Swiss National Science Foundation (2000-063818) and the Portuguese Science and Technology Foundation (PTDC/ECM/65442/2006).

References

Bathurst J. C., Li R. M. and Simons D. B. (1981) Resistance equation for large-scale roughness, *J. Hydraul. Eng. ASCE*, **107** (12), 1593–1613.

Bathurst J. C. (1988) Velocity profile in high-gradient, boulder-bed channels, *Proc. Int. Conf. on Fluvial Hydraulics IAHR*, 29–34, Budapest, Hungary.

Buffin-Bélanger T. and Roy A. G. (1998) Effects of a pebble cluster on the turbulent structure of a depth-limited flow in a gravel-bed river, *Geomorphology*, **25**, 249–267.

Ferro V. and Baiamonte G. (1994) Flow velocity profiles in gravel-bed rivers, *J. Hydraul. Eng. ASCE*, **120** (1), 60–80.

Franca M. J. (2005a) Flow dynamics over a gravel riverbed, *Proc. XXXI IAHR Congress IAHR*, 6542–6551, Seoul, South Korea.

Franca M. J. (2005b) *A field study of turbulent flows in shallow gravel-bed rivers,* PhD dissertation No. 3393, École Polytechnique Fédérale de Lausanne (http://library.epfl.ch/theses/?nr=3393), Lausanne, Switzerland.

Franca M. J. and Lemmin U. (2004) A field study of extremely rough, three-dimensional river flow, *Proc. 4thInt. Symp. on Environmental Hydraulics IAHR*, 107–112, Hong Kong.

Franca M. J. and Lemmin U. (2005) Cross-section periodicity of turbulent gravel-bed river flows, *Proc. 4thRiver Coastal and Estuarine Morphodynamics IAHR*, 203–210, Urbana, Illinois, USA.

Franca M. J. and Lemmin U. (2006) Eliminating velocity aliasing in acoustic Doppler velocity profiler data, *Meas. Sci. Technol.*, **17** (2), 313–322.

Katul G., Wiberg P., Albertson J. and Hornberger G. (2002) A mixing layer theory for flow resistance in shallow streams, *Water Resour. Res.*, **38** (11), 1250.

Marchand J. P., Jarrett R. D. and Jones L. L. (1984) Velocity profile, surface slope, and bed material size for selected streams in Colorado, *US Geol. Survey Open File Report 84–733.*

Monin A. S. and Yaglom A. M. (1971) *Statistical Fluid Mechanics: Mechanics of Turbulence*, Vol. 1, The MIT Press, Cambridge, Massachusetts, USA.

Morris H. M. (1959) Design methods for flow in rough conduits, *J. Hydraul. Eng. ASCE*, **85** (7), 43–62.

Nelson J. M., McLean S. R. and Wolfe S. R. (1993) Mean flow and turbulence fields over two-dimensional bed forms, *Water Resour. Res.*, **29** (12), 3935–3953.

Nikora V. and Smart G. M. (1997) Turbulence characteristics of New Zealand gravel-bed rivers, *J. Hydraul. Eng. ASCE*, **123** (9), 764–773.

Nikora V. and Goring D. (2000) Flow turbulence over fixed and weakly mobile gravel beds, *J. Hydraul. Eng. ASCE*, **126** (9), 679–690.

Rolland T. and Lemmin U. (1997) A two-component acoustic velocity profiler for use in turbulent open-channel flow, *J. Hydraul. Res.*, **35** (4), 545–561.

Roy A. G., Buffin-Belanger T., Lamarre H. and Kirkbride A. D. (2004) Size, shape and dynamics of large-scale turbulent flow structures in a gravel-bed river, *J. Fluid Mech.*, **500**, 1–27.

Schlichting H. (1968) *Boundary-Layer Theory*, McGraw-Hill, New York, New York, USA.

Shen C. and Lemmin U. (1997) Ultrasonic scattering in highly turbulent clear water flow, *Ultrasonics*, **35** (1), 57–64.

Wolman M. G. (1954) A method of sampling coarse river-bed material, *Trans. Amer. Geoph. Un.*, **35** (6), 951–956.